NASA TECHNICAL NOTE

NASA TN D-3282

NASA TN D-3282

EFFECT OF NOSE-MOUNTED CONTROL-SYSTEM JETS IN ROLL-CONTROL POSITIONS ON THE AERODYNAMICS OF A SPACE VEHICLE

by John T. Suttles and Robert L. James, Jr.

Langley Research Center
Langley Station, Hampton, Va.

NATIONAL AERONAUTICS AND SPACE ADMINISTRATION • WASHINGTON, D. C. • FEBRUARY 1966

NASA TN D-3282

EFFECT OF NOSE-MOUNTED CONTROL-SYSTEM JETS IN ROLL-CONTROL POSITIONS ON THE AERODYNAMICS OF A SPACE VEHICLE

By John T. Suttles and Robert L. James, Jr.

Langley Research Center
Langley Station, Hampton, Va.

NATIONAL AERONAUTICS AND SPACE ADMINISTRATION

For sale by the Clearinghouse for Federal Scientific and Technical Information
Springfield, Virginia 22151 – Price $2.00

EFFECT OF NOSE-MOUNTED CONTROL-SYSTEM JETS IN ROLL-CONTROL POSITIONS ON THE AERODYNAMICS OF A SPACE VEHICLE

By John T. Suttles and Robert L. James, Jr.
Langley Research Center

SUMMARY

A wind-tunnel investigation has been conducted to determine the effect of jets produced by a nose-mounted solid-rocket control system on the aerodynamics of a two-stage rocket vehicle. The configuration tested was a 0.10-scale model of an NASA flight research vehicle consisting of a first stage composed of a fin-stabilized booster with two auxiliary rockets and a second stage composed of a rocket motor with a spacecraft compartment mounted on its forward end. The solid-rocket control system is housed within the spacecraft compartment. This configuration was tested in the Langley Unitary Plan wind tunnel by exhausting cold air from simulated control-rocket nozzles. The tests were conducted for the roll-control mode at a Mach number of 2.80 with variations in the angle of attack and the jet-to-free-stream pressure ratio.

The results of this investigation indicate that significant aerodynamic effects are obtained when the control system is used in conjunction with downstream fins and auxiliary rockets. It was found that use of the roll-control mode for this configuration could result in a sizable loss of control power; in addition, it was found that a small reduction of static stability was obtained.

INTRODUCTION

The National Aeronautics and Space Administration has undertaken a general program to evaluate various rocket vehicle control-system concepts. One such control system used in conjunction with a two-stage rocket vehicle is described in reference 1. The vehicle described in reference 1 consists of two stages with a spacecraft compartment mounted at the forward end of the second stage. Housed within this spacecraft compartment is the control system which uses the thrust of four auxiliary solid-propellant rockets for control forces. These rockets are arranged so that they may be rotated to produce pitch-, yaw-, and roll-control moments.

The control system is employed at high altitudes, thus, an exhaust plume is formed at the exit of each of the four control-rocket nozzles. The presence of jet plumes such as these can produce significant flow separation ahead of the jets and thereby affect the aerodynamic characteristics of the body. This effect has been explored for single jets exhausting at the rear of missile-type

bodies in references 2 to 5. In addition, jets exhausting over adjacent surfaces can greatly affect the pressure distribution over these surfaces and cause induced aerodynamic effects. (See refs. 6 to 13, for example.) Another problem area which exists and is of particular concern for the nose-mounted control system is the effect of the control-rocket exhaust on the downstream flow field when these rockets are rotated to produce control moments or when the body is at an angle of attack.

Because of the complexity of the aforementioned phenomena, it would be extremely difficult to determine analytically the effect of the control jets on the aerodynamics of the rocket vehicle considered herein. Therefore, a wind-tunnel investigation was undertaken to explore these problem areas, the results of which are the subject of the present report. The control system was originally designed to control only the second stage of an NASA flight research vehicle. (See ref. 1.) However, a study was conducted to determine the feasibility of employing the system in roll control prior to first-stage separation. Therefore, the wind-tunnel test program presented herein was conducted for two model configurations, namely the complete configuration and the configuration with the stabilizing fins and auxiliary rockets removed. Only roll-control deflections were utilized and a representative Mach number of 2.80 was selected for these tests which were conducted on a 0.10-scale model in the Langley Unitary Plan wind tunnel. The hot exhaust gases of the full-scale control rockets were simulated with cold air. The jet-to-free-stream pressure ratio, the control-rocket deflection angles, and body angle of attack were varied during the investigation.

SYMBOLS

The coefficients of forces and moments are referred to the body-axis system. (See fig. 1.) Aerodynamic moments presented are referenced to a moment center located 21.60 inches (0.549 m) back of the theoretical nose apex of the model as shown in figure 2. Coefficients are based on the first-stage body diameter of 3.10 inches (0.0787 m) and a corresponding area of 7.55 sq in. ($0.0049\ m^2$).

Measurements for this investigation were taken in the U.S. Customary System of Units. Equivalent values are indicated herein in the International System of of Units (SI) in the interest of promoting use of this system in future NASA reports.

A_j nozzle exit area, sq in. (m^2)

A_t nozzle throat area, sq in. (m^2)

C_l rolling-moment coefficient, $\frac{l}{qSd}$

C_m pitching-moment coefficient, $\frac{m}{qSd}$

C_N normal-force coefficient, $\frac{F_N}{qS}$

d diameter of first stage of test configuration, in. (m)

d_j nozzle exit diameter, in. (m)

l rolling moment, in-lb (N·m)

m pitching moment, in-lb (N·m)

M_∞ free-stream Mach number

M_j jet Mach number at nozzle exit

F_N normal force, lb (N)

p_j jet static pressure at nozzle exit, lb/sq ft (N/m^2)

p_∞ ambient or free-stream static pressure, lb/sq ft (N/m^2)

q free-stream dynamic pressure, lb/sq in. (N/m^2)

S cross-sectional area of first stage of test configuration, sq in. (m^2)

α angle of attack of model center line, deg

δ_j angle between jet axis and tangent to free jet boundary at nozzle lip, that is, initial inclination of jet boundary, deg (See fig. 4.)

δ control rocket deflection angle, deg (See following sketch.)

γ_j ratio of specific heats in rocket exhaust

θ_n divergence angle of conical nozzle, deg (See fig. 4.)

X,Y,Z body-axis system

Subscripts:

1,2,3,4 control rocket number as shown in following sketch which also shows the deflection angle δ for rocket 4

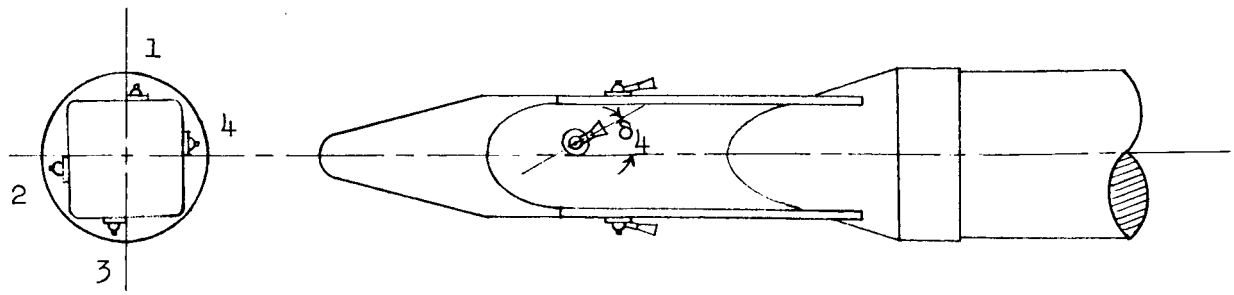

APPARATUS AND TESTS

Wind Tunnel

This investigation was conducted in the Langley Unitary Plan wind tunnel at a free-stream Mach number of 2.80. This facility is described in reference 14.

Model

Model details and dimensions are presented in figure 2 and a photograph of the nose section is shown in figure 3. The model is a 0.10-scale model of the flight research vehicle described in reference 1. The flight vehicle configuration consists of a fin-stabilized booster with two auxiliary rockets to give additional take-off acceleration and a second stage composed of a rocket motor with a spacecraft compartment mounted on its forward end. A control system composed of four end-burning solid-propellant rockets is contained in the spacecraft compartment and the control-rocket nozzles protrude from the spacecraft skin. Details of the model control-rocket nozzle are shown in figure 2(b).

The first stage is equipped with a cruciform arrangement of modified double-wedge fin panels, one of which is shown in detail in figure 2(c). The fin panel had an aspect ratio of 1.5 and represented full-scale panels of 12 square feet $(1.11\ m^2)$. The model was mounted in the tunnel so that the planes formed by the fin panels made an angle of 45° with the pitch and yaw axes. The first-stage auxiliary rocket motors, shown mounted on the vehicle in figure 2(a), are shown in detail in figure 2(c).

In order to simulate the exhaust of the control rockets, a high-pressure plenum chamber was provided inside the model nose. A high-pressure air supply line and a pressure monitoring tube were attached to the model support sting and were run into the rear of the model, around the balance, through a slot in the model and up to the plenum chamber at the nose. Details of the air supply system and balance installation are shown in figure 2(d). During the tests

reported herein, the aft balance moment center location was used. (See fig. 2(d).) However, to be compatible with data previously obtained for this configuration (see ref. 15), all moment data presented have been converted to the forward moment center location.

Instrumentation

Aerodynamic forces and moments were determined by means of a six-component electrical strain-gage balance; however, only data from the rolling-moment, pitching-moment, and normal-force components are presented. The balance was housed within the body of the model and was rigidly fastened to the sting support (fig. 2(d)). The pressure-monitoring tube connected the plenum chamber in the model to an externally located pressure transducer.

Control-Rocket Jet Simulation

The full-scale control rockets have supersonic, convergent-divergent, conical nozzles and have hot gas exhausts (solid propellant) with a ratio of specific heats γ_j of 1.23. These control rockets are employed in flight at high altitudes so that p_j/p_∞ varies on the order of from 10^2 to 10^6. At these high values of p_j/p_∞, a large jet plume is formed at the exit of each of the control-rocket nozzles. It is important to simulate these large jet boundaries in the wind-tunnel tests because their size is an important factor for each of the two potential problem areas being studied in this investigation. One of these potential problem areas is associated with the aerodynamic effects resulting from flow separation ahead of the jets and the other is concerned with the aerodynamic effects resulting from the influence of the control-rocket exhaust on the downstream flow field. The large jet plumes are important since the size of the jet boundaries will determine the degree of separated flow ahead of the jets and will affect the extent of the influence of the jets on the downstream flow field.

In the wind-tunnel tests, room-temperature (70° F (294° K)) air was used in the model nozzles to simulate the full-scale rocket jets. To account for the difference in γ_j between the hot gas and air (γ_j = 1.23 and 1.40, respectively), a relationship given in reference 16 as

$$\left(\frac{\gamma_j M_j^2}{\sqrt{M_j^2 - 1}}\right)_{\text{Model}} = \left(\frac{\gamma_j M_j^2}{\sqrt{M_j^2 - 1}}\right)_{\text{Full scale}}$$

was satisfied in the test nozzle design. The use of this relationship resulted in air nozzles for the wind-tunnel model with $M_j = 3.36$.

Previous tests and calculations (ref. 17) have shown that, when jet boundaries are simulated, the most important property to be duplicated is the initial

inclination angle of the jet (δ_j). This initial angle is affected by the values of γ_j, M_j, θ_n, M_∞, and p_j/p_∞. Therefore, in order to simulate the initial inclination angles of the control-rocket jet plumes with the attainable values of γ_j and p_j/p_∞, the test nozzles were designed with θ_n greater than that of the full-scale control-rocket nozzles. The initial jet inclination angles for the model and full-scale rocket nozzles were calculated by two-dimensional theory. The calculations were performed only for cases of large δ_j so that the assumption of separated flow ahead of the jet could be used in the same manner as in reference 17. It was also assumed that the pressure rise across an oblique shock with 30° turning (see ref. 17) occurs at separation where the upstream Mach number is the same as the free-stream Mach number. From these calculations, it was determined that in order to simulate even in a modest way the large values of δ_j with the restricted values of γ_j and p_j/p_∞, the nozzle divergence angle θ_n should be 50° for the control rockets on the model.

The relationships of δ_j to p_j/p_∞ for the full-scale nozzles and for the test nozzle are shown in figure 4. It can be seen in this figure that the test nozzles will provide δ_j values from about 50° to 73° for values of p_j/p_∞ of approximately 6 to 70 which correspond to full-scale values of p_j/p_∞ of about 230 to 13 000, respectively.

While the duplication of the initial inclination angle of the jet (δ_j) between the model and the full-scale configuration is adequate for simulation of the condition affecting the flow separation ahead of the jet, it is not adequate for simulation of the downstream jet conditions. The downstream jet characteristics are not only affected by the initial jet angle but also depend on the mixing between the jet and free-stream flows and on the jet momentum. In the tunnel test described herein it was not possible to match the parameters which provide a simulation of the jet free-stream mixing and jet momentum. Based on considerations such as those given in reference 16, it appears that exact simulation of these conditions will require tests with hot-jet exhaust gases and duplication of the large p_j/p_∞ values.

In view of these facts, test results in this report which are affected by downstream jet characteristics should be used only to establish trends for full-scale effects.

Compared in the following table are the characteristics of the full-scale control rocket nozzle and the test nozzles:

Characteristic	Full-scale	Test
γ_j	1.23	1.40
M_j	3.89	3.36
θ_n	15°	50°
A_j/A_t	20	5.96
d_j	2.362 in. (0.06 m)	0.2362 in. (0.006 m)

Tests and Procedure

Tests were conducted for the complete model configuration and for the model configuration with the first-stage stabilizing fins and auxiliary rockets removed. All tests were run at a free-stream Mach number of 2.80 and the angle of attack was varied from approximately -8° to 8° at zero angle of sideslip.

The control rockets were positioned to produce various negative roll-control moments. For the jet-on conditions all four motors were exhausting while either two or four nozzles were deflected to produce the control moments. The plenum chamber pressure (assumed to be jet stagnation pressure) was recorded along with the free-stream static pressure for each run. The jet static pressure was calculated from the isentropic nozzle flow relationship between area and pressure ratios; the pressure ratio p_j/p_∞ was determined in this manner for each test condition. A complete list of the tests conducted is shown in table I.

Corrections to Experimental Data

Model asymmetries.- The experimental data presented in this report have been corrected for model misalinements and asymmetries by shifting all data the amount required to make C_N, C_m, and C_l values zero at zero angle of attack with the jets off. This correction was made independently for each configuration and control-moment deflection condition, so that aerodynamic effects created by the rocket nozzles (without jet flow) were removed from the data presented, along with the effects of model fin misalinements and other asymmetries. These adjustments in the data were very small.

Control rocket thrust.- In order to remove the control-rocket thrust contributions from the aerodynamic coefficients accurately, special tests were made for each configuration and control-rocket deflection combination considered herein. During these tests the model was mounted in the tunnel in the normal manner, but there was no tunnel flow ($q = 0$), therefore the aerodynamic effects were eliminated from the data obtained. The pressure in the wind-tunnel test section was reduced so that p_∞ values were obtained which compared with those present during the regular test program. The plenum chamber pressure was also varied to provide the range of values of p_j used in the regular tests. (See table I.) The l, m, and F_N values recorded for the various p_j values used were later changed to coefficients by using the proper values for q, S, and d and taken out of the experimental data presented herein. Thus, the values for the coefficients C_l, C_m, and C_N presented do not include the contributions produced by the control rocket thrust with no wind-tunnel flow.

Accuracy

As described previously, pressure-supply and pressure-monitoring tubes were run from outside the model through the rear and to the plenum chamber in the nose. Balance calibrations were made to determine whether these tubes

would cause erroneous measurements. During these calibrations, the tubes were pressurized to the values used in the wind-tunnel tests; known forces and moments were applied to the model and balance measurements were recorded. Comparisons were made of the forces and moments measured by the balance and those applied to the model and were found to agree within the quoted accuracy of the balance. (See values of l, m, and F_N in the following list.) It was therefore concluded that the tubing caused an insignificant effect on the balance measurements.

The estimated maximum inaccuracies of the coefficients and other pertinent parameters measured herein, based on instrument calibration and data repeatability, are as follows:

C_l	±0.02
C_m	±0.12
C_N	±0.14
l	±0.5 in-lb (±0.0565 N·m)
m	±4.0 in-lb (±0.4519 N·m)
F_N	1.5 lb (6.672 N)
α	±0.1°
p_j/p_∞	±4 percent

RESULTS

Results of the investigation are presented in figures 5 to 7 in plots showing the variation of C_N, C_m, and C_l with angle of attack. Data are presented in most of the plots for the jet-off and jet-on conditions. Therefore direct comparisons can be made to determine induced aerodynamic effects due to the control-rocket jets. Any differences in the data for the jet-off and jet-on conditions are induced aerodynamic effects since the control-rocket thrust effects have been removed from all data presented.

Effect of p_j/p_∞

Data are presented in figure 5 to show the effect of jet-pressure ratio p_j/p_∞ on the aerodynamic characteristics of the complete configuration. In figure 5(a) the results are given for two control rockets deflected to produce negative roll-control moments. The jet-off data show linear variations of C_N and C_m with angle of attack near zero and no significant values of C_l through the angle-of-attack range of these tests. Similar results were also shown in reference 15 for this configuration.

In examining the jet-on data, it is immediately apparent that induced values of C_l are obtained for these conditions. The shape of the curves produced by the induced roll moments varies appreciably with p_j/p_∞. At zero

angle of attack the induced values increase with increasing p_j/p_∞, but at the higher angles of attack the effect of p_j/p_∞ is not clearly defined. The C_N and C_m data show no noticeable induced effects for this configuration except for a small nonlinear trend in C_m at the highest p_j/p_∞.

In figure 5(b) the results are given for all four control rockets deflected 30° to produce negative roll-control moments. The C_l data again indicate noticeable positive induced roll moments. However, these data have a more regular decreasing trend with angle of attack and more uniform variation with p_j/p_∞ than the data for two control rockets deflected (fig. 5(a)). The C_N data show no noticeable effects due to control-rocket exhaust. The C_m data do have noticeable changes in the linearity, and at the highest p_j/p_∞ value a small destabilizing effect (reduction in slope of curve of C_m plotted against α) is apparent at zero angle of attack.

Effect of Fins and Auxiliary Rockets

In order to investigate the origin of the induced effects obtained, tests were conducted with fins and auxiliary rockets removed. The results of these tests are presented in figure 6. The jet-on and jet-off data for this configuration indicate no measurable effects due to the control-rocket jets.

Effect of Control-Rocket Deflection Angle

Data are presented in figure 7 for the complete configuration with all four rockets in the neutral position and with all four rockets deflected at various angles to produce negative roll moments. These data again indicate noticeable induced effects in the C_l data which decrease at angles of attack. These results also show that an increase in control-rocket deflection angle will result in an increase in the induced roll moment. The variations in C_N with angle of attack show no apparent effects due to control deflection. The C_m data do show nonlinear variations near zero angle of attack which tend to decrease the static stability (reduction in slope of the curve of C_m plotted against α). This effect, however, shows no uniform variation with control deflection.

DISCUSSION

It is important to note that, although the controls were deflected to produce negative control moments, the induced values of C_l obtained were positive. Consequently, a decrease in roll-control effectiveness will result. A comparison of the results for the complete configuration with those for the configuration without fins and auxiliary rockets shows that the induced effects are associated with the fins and auxiliary rockets. The mechanism which is

probably involved is that of a downwash field being generated by the control-rocket jets and the impingement of this induced flow field on the fins and auxiliary rockets at the rear of the configuration. This effect is similar to that caused by upper-stage fins where the downwash produces induced aerodynamic forces on downstream body surfaces and fins.

Since it has been established that the induced effects are associated with the presence of the fins and auxiliary rockets, the simulation of the downstream characteristics of the jet becomes of primary importance. It was pointed out in the description of the jet simulation that a simulation of the downstream characteristics of the jets was not obtained. Therefore the results of this investigation must be considered as establishing trends only.

In figure 8 the induced-roll-moment data are presented as the ratio of the induced roll moment to the corresponding applied thrust moment. Presenting the data in this manner not only gives a direct measure of the effectiveness of the control rockets of the test configuration but also tends to account for the lack of simulation of the jet momentum. The jet-momentum effects tend to be canceled because the thrust moment is directly affected by the momentum of the exhaust jet and, from all indications, the induced moments would be also. It is apparent from the data that the induced roll moments are quite significant. For example, at the lowest p_j/p_∞ value for the configuration with two rockets deflected to produce roll moments and at angles of attack between about -4° and -7.5°, a control reversal will result. Near zero angle of attack the induced moments do not vary appreciably with p_j/p_∞, however, at angles of attack variations are obtained. The most severe control degradation occurs for the configuration with two rockets deflected and at the lower values of p_j/p_∞. The least effect is in general obtained at the highest angles of attack for the highest p_j/p_∞ values. No reasonable explanation has been found for the large change in the induced moments at angles of attack between the highest and lowest p_j/p_∞ conditions for the configuration with two rockets deflected. However, it appears reasonable that the induced moments would decrease as angle of attack is increased because the fins tend to be displaced from the wake generated by the control-rocket jets. Changes in the control-rocket deflection angle from 30° to 60° appeared to have little or no effect on the ratio of induced moment to control-rocket thrust moment.

The data presented do not provide sufficient information to determine the cause of the small changes in linearity of the C_m data. This effect could be caused by a disruption of the flow over the fins and/or by flow separation at the nose. The effect is small, however, and a complete explanation of its causes does not appear to be important.

CONCLUDING REMARKS

The results of a wind-tunnel investigation of the effect of nose-mounted control system jets in roll-control positions on the aerodynamics of a two-stage fin-stabilized rocket vehicle have shown that significant aerodynamic effects

are obtained. Induced roll moments will result from use of the roll-control mode which may be quite large and are in a direction which reduces effectiveness of the control rockets. The induced roll is associated with the fins and auxiliary rockets at the base of the vehicle and is probably caused by a downwash field generated by the control-rocket jets. The control-rocket jets also cause a nonlinear variation of pitching moment with angle of attack near zero, which results in a slightly lower static-stability level.

The use of a nose-mounted control system in conjunction with surfaces such as fins, auxiliary rockets, and other protuberances should be approached with much caution. Due to the nature of the problem, each new configuration should be separately examined to assess the aerodynamic effects.

Langley Research Center,
National Aeronautics and Space Administration,
Langley Station, Hampton, Va., October 10, 1965.

REFERENCES

1. Young, A. Thomas; and Harris, Jack E.: An Analog Study of a Rotating-Solid-Rocket Control System and Its Application to Attitude Control of a Space-Vehicle Upper Stage. NASA TN D-2366, 1964.

2. Fetterman, David E., Jr.: Effects of Simulated Rocket-Jet Exhaust on Stability and Control of a Research-Type Airplane Configuration at a Mach Number of 6.86. NASA TM X-127, 1959.

3. Salmi, Reino J.: Effects of Jet Billowing on Stability of Missile-Type Bodies at Mach 3.85. NASA TN D-284, 1960.

4. Falanga, Ralph A.; Hinson, William F.; and Crawford, Davis H.: Exploratory Tests of the Effects of Jet Plumes on the Flow Over Cone-Cylinder-Flare Bodies. NASA TN D-1000, 1962.

5. Hinson, William F.; and Falanga, Ralph A.: Effect of Jet Pluming on the Static Stability of Cone-Cylinder-Flare Configurations at a Mach Number of 9.65. NASA TN D-1352, 1962.

6. Bressette, Walter E.: Investigation of the Jet Effects on a Flat Surface Downstream of the Exit of a Simulated Turbojet Nacelle at a Free-Stream Mach Number of 2.02. NACA RM L54E05a, 1954.

7. Englert, Gerald W.; Wasserbauer, Joseph F.; and Whalen, Paul: Interaction of a Jet and Flat Plate Located in an Airstream. NACA RM E55G19, 1955.

8. Bressette, Walter E.; and Leiss, Abraham: Investigation of Jet Effects on a Flat Surface Downstream of the Exit of a Simulated Turbojet Nacelle at a Free-Stream Mach Number of 1.39. NACA RM L55L13, 1956.

9. Bressette, Walter E.: Some Experiments Relating to the Problem of Simulation of Hot Jet Engines in Studies of Jet Effects on Adjacent Surfaces at a Free-Stream Mach Number of 1.80. NACA RM L56E07, 1956.

10. Leiss, Abraham; and Bressette, Walter E.: Pressure Distribution Induced on a Flat Plate by a Supersonic and Sonic Jet Exhaust at a Free-Stream Mach Number of 1.80. NACA RM L56I06, 1957.

11. Bressette, Walter E.; and Leiss, Abraham: Effects on Adjacent Surfaces From the Firing of Rocket Jets. NACA RM L57D19a, 1957.

12. Falanga, Ralph A.; and Janos, Joseph J.: Pressure Loads Produced on a Flat-Plate Wing by Rocket Jets Exhausting in a Spanwise Direction Below the Wing and Perpendicular to a Free-Stream Flow of Mach Number 2.0. NASA TN D-893, 1961. (Supersedes NACA RM L58D09.)

13. Leiss, Abraham: Pressure Distribution Induced on a Flat Plate at a Free-Stream Mach Number of 1.39 by Rockets Exhausting Upstream and Downstream. NASA TN D-1507, 1962. (Supersedes NASA TM X-129.)

14. Anon.: Manual for Users of the Unitary Plan Wind Tunnel Facilities of the National Advisory Committee for Aeronautics. NACA, 1956.

15. Suttles, John T.: Aerodynamic Characteristics From Mach 0.22 to 4.65 of a Two-Stage Rocket Vehicle Having an Unusual Nose Shape. NASA TN D-2163, 1964.

16. Pindzola, M.: Jet Simulation in Ground Test Facilities. AGARDograph 79, Nov. 1963.

17. Love, Eugene S.; Grigsby, Carl E.; Lee, Louise P.; and Woodling, Mildred J.: Experimental and Theoretical Studies of Axisymmetric Free Jets. NASA TR R-6, 1959. (Supersedes NACA RM L54L31 by Love and Grigsby, RM L55J14 by Love, RM L56G18 by Love, Woodling, and Lee, and TN 4195 by Love and Lee.)

TABLE I.- PRESENTATION OF TEST CONDITIONS

[All tests were run at a Mach number of 2.80 for an angle-of-attack range of approximately -8° to 8° at zero angle of sideslip]

Test	Configuration	Control rocket deflections (for negative roll moments)	p_j		$\frac{p_j}{p_\infty}$
			psf	N/m^2	
1	Complete	$\delta_1 = \delta_3 = 45°$; $\delta_2 = \delta_4 = 0°$	Jet off		
2	↓	↓	2450	117 306	15
3			2450	117 306	23
4			2450	117 306	45
5			2450	117 306	67
6		$\delta_1 = \delta_2 = \delta_3 = \delta_4 = 30°$	1600	76 608	15
7		↓	1600	76 608	30
8	↓		1600	76 608	40
9	Fins and auxiliary rockets removed	$\delta_1 = \delta_3 = 45°$; $\delta_2 = \delta_4 = 0°$	Jet off		
10	↓	↓	1100	52 668	28
11			1600	76 608	40
12	Complete	$\delta_1 = \delta_2 = \delta_3 = \delta_4 = 0°$	1600	76 608	40
13	↓	$\delta_1 = \delta_2 = \delta_3 = \delta_4 = 60°$	1600	76 608	40

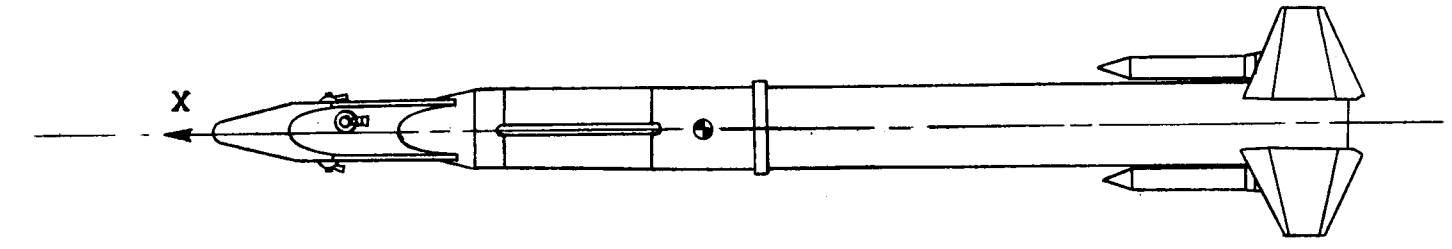

TOP VIEW

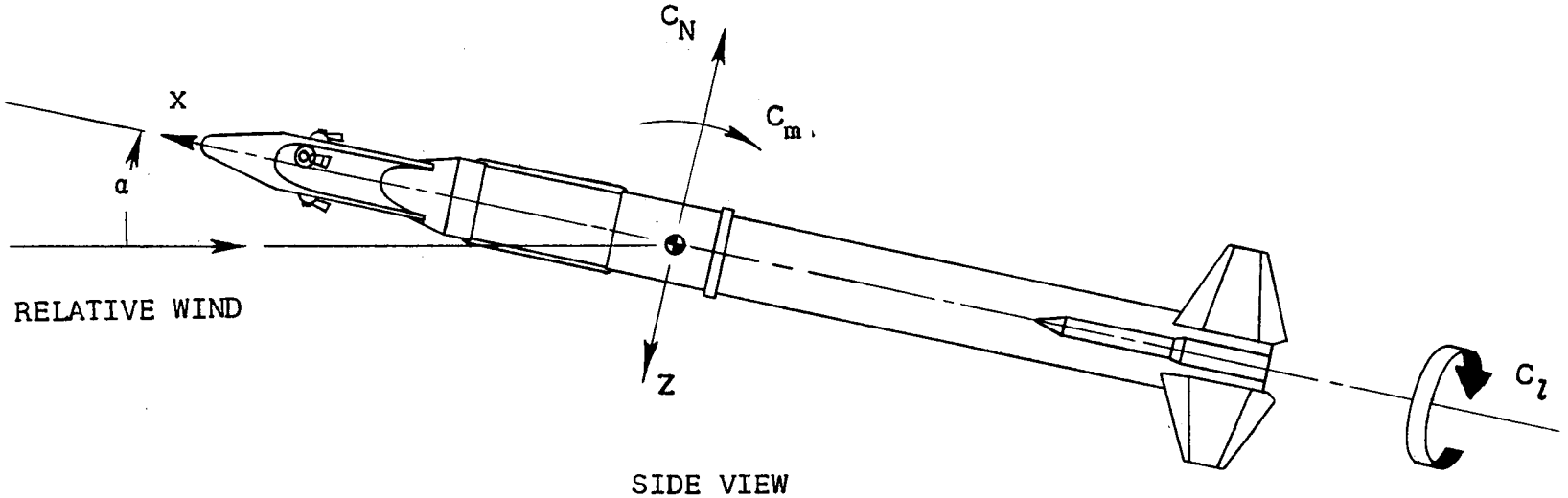

SIDE VIEW

Figure 1.- Body-axis system. Arrows indicate positive directions.

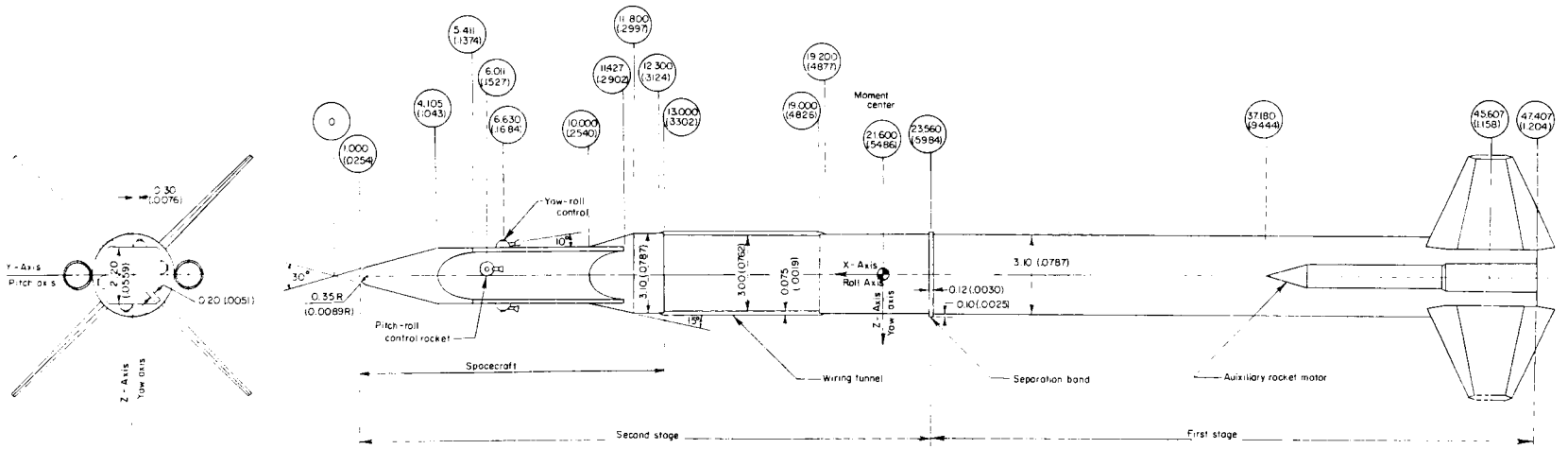

(a) Complete configuration. Circled numbers indicate model station in inches (meters).

Figure 2.- Details and dimensions of 0.10-scale model. Linear dimensions are given first in inches and parenthetically in meters.

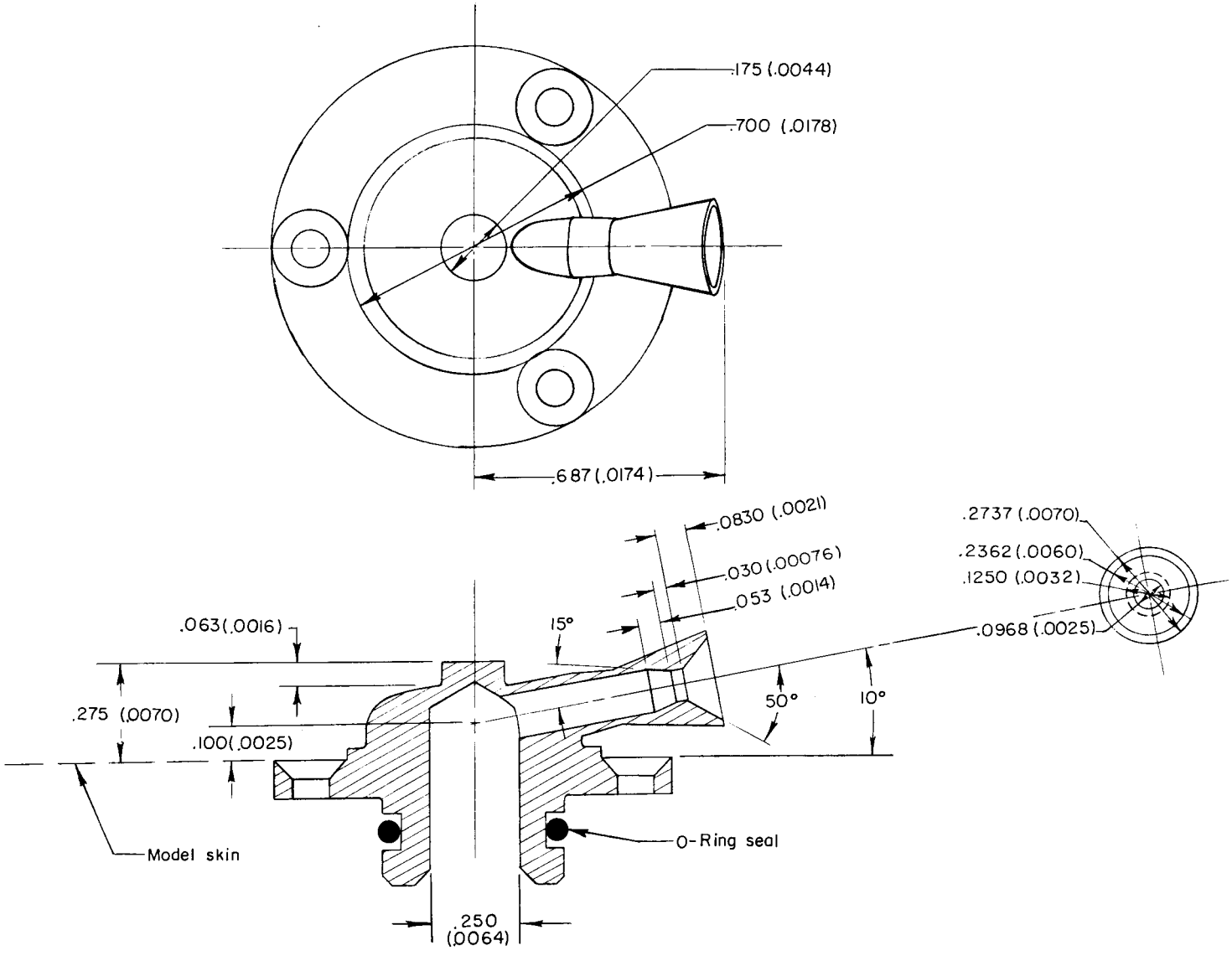

(b) Control rocket nozzle.

Figure 2.- Continued.

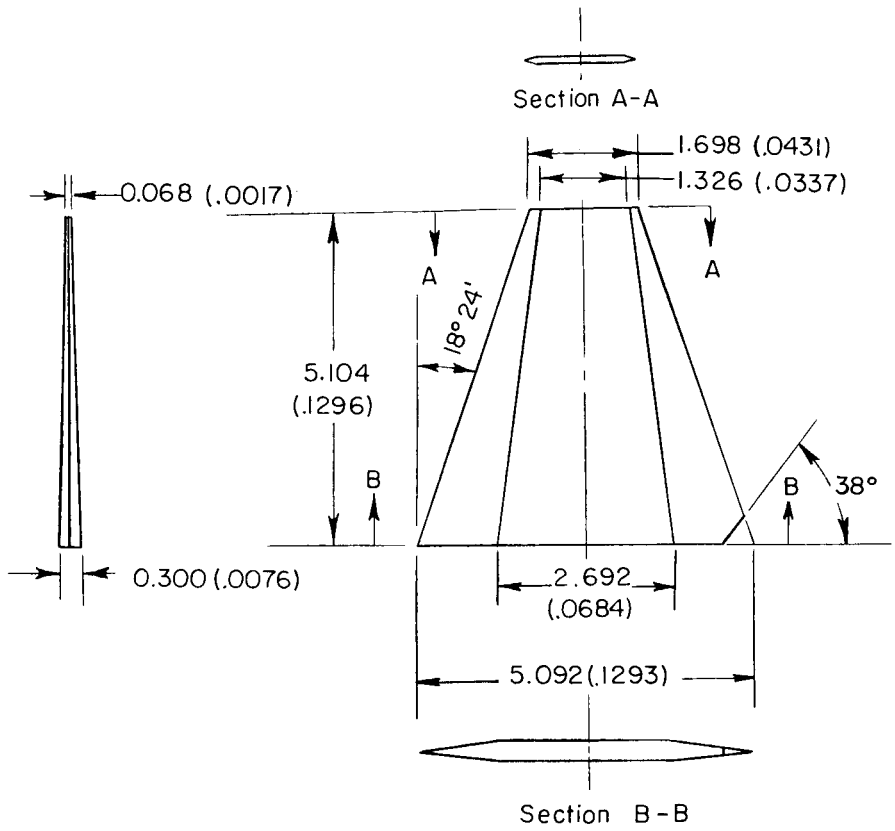

Fin panel

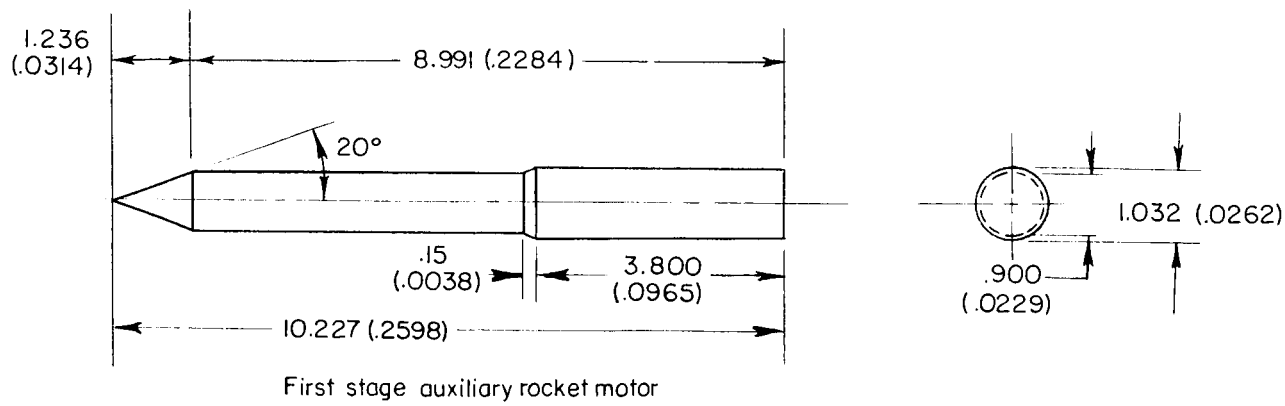

First stage auxiliary rocket motor

(c) Fin panel and first-stage auxiliary rocket motor.

Figure 2.- Continued.

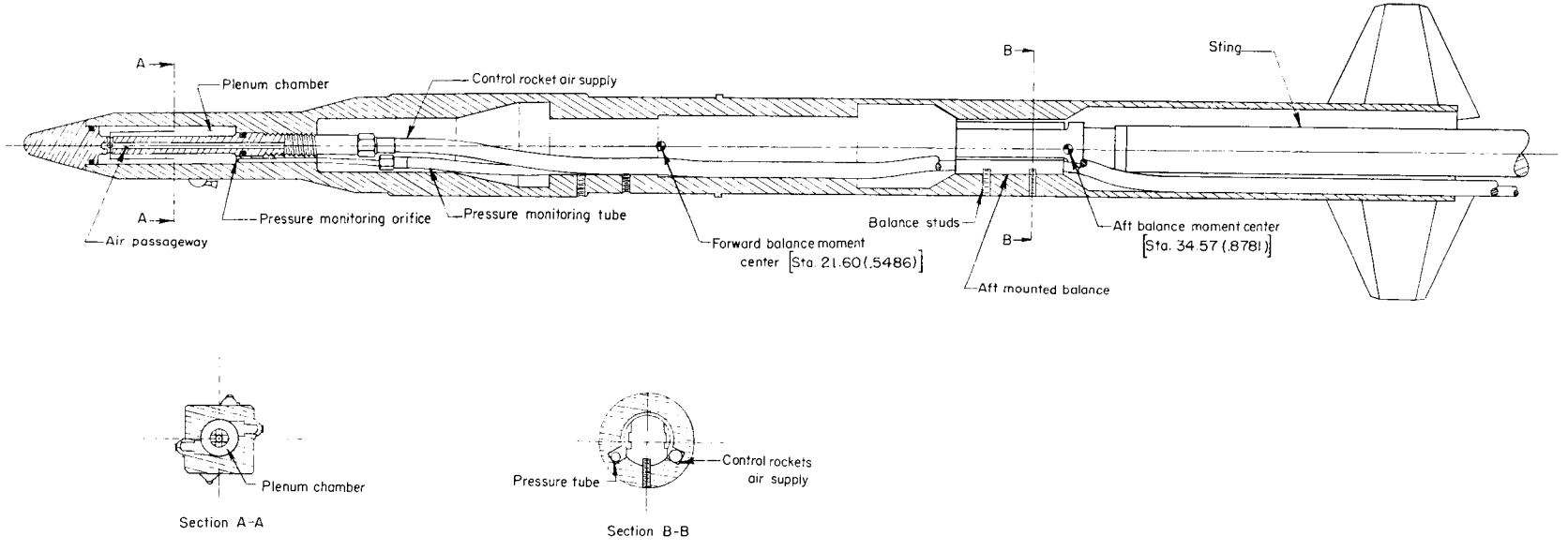

(d) Control-rocket air supply system and balance installation.

Figure 2.- Concluded.

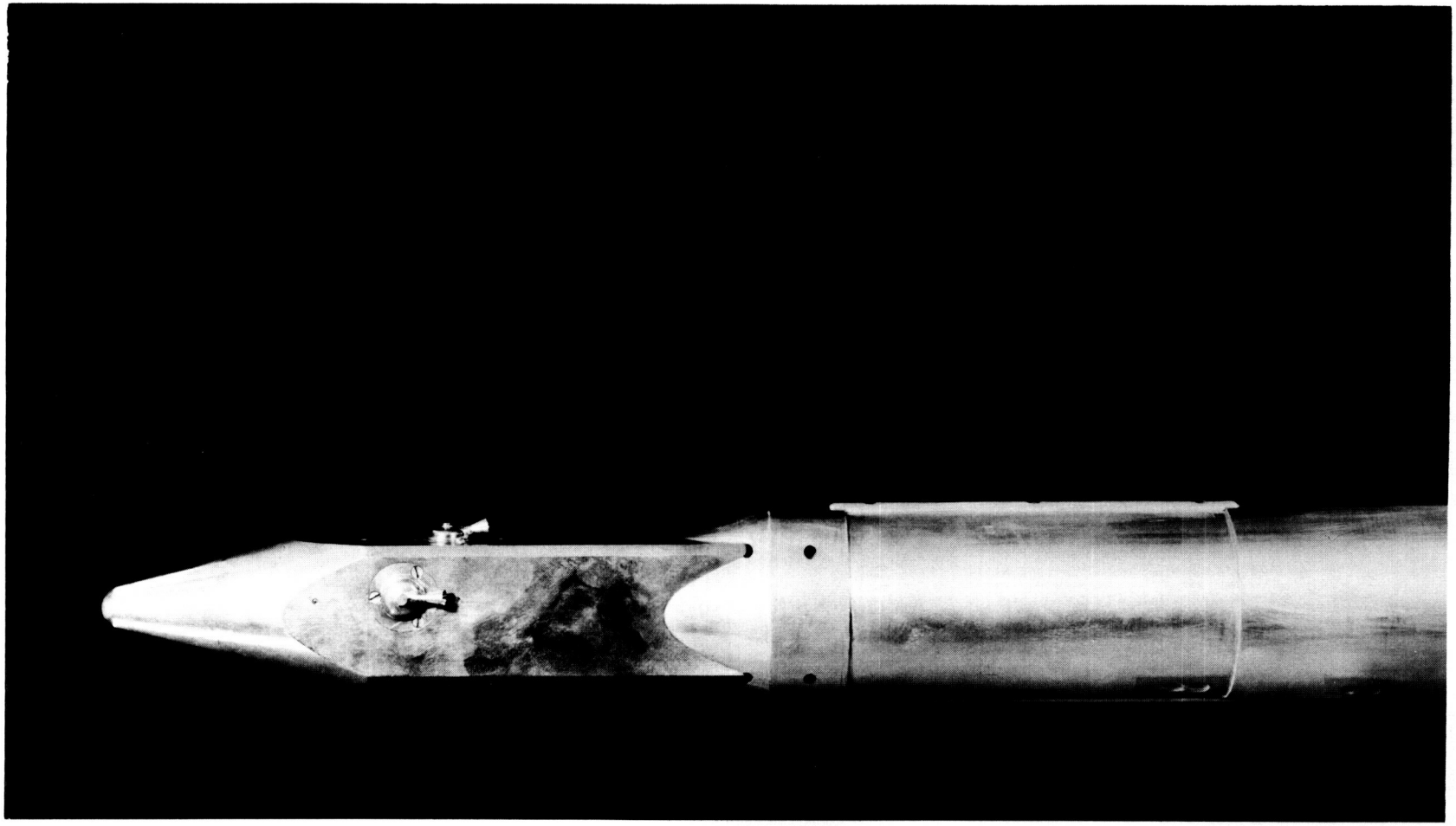

Figure 3.- Photograph of model nose section.

L-62-7993

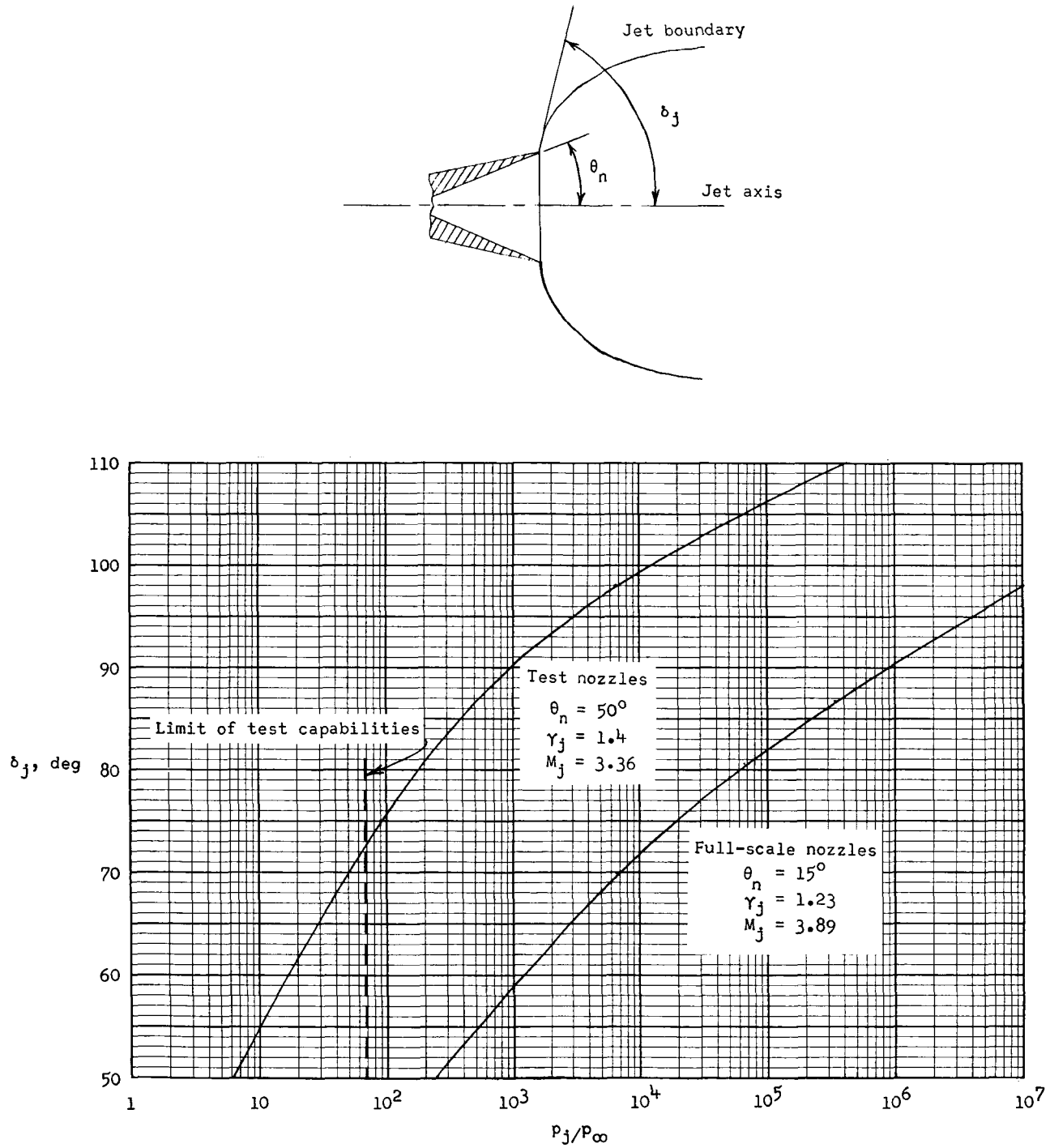

Figure 4.- Comparison of initial jet-boundary slopes of the full-scale control-rocket nozzles and the test nozzles.

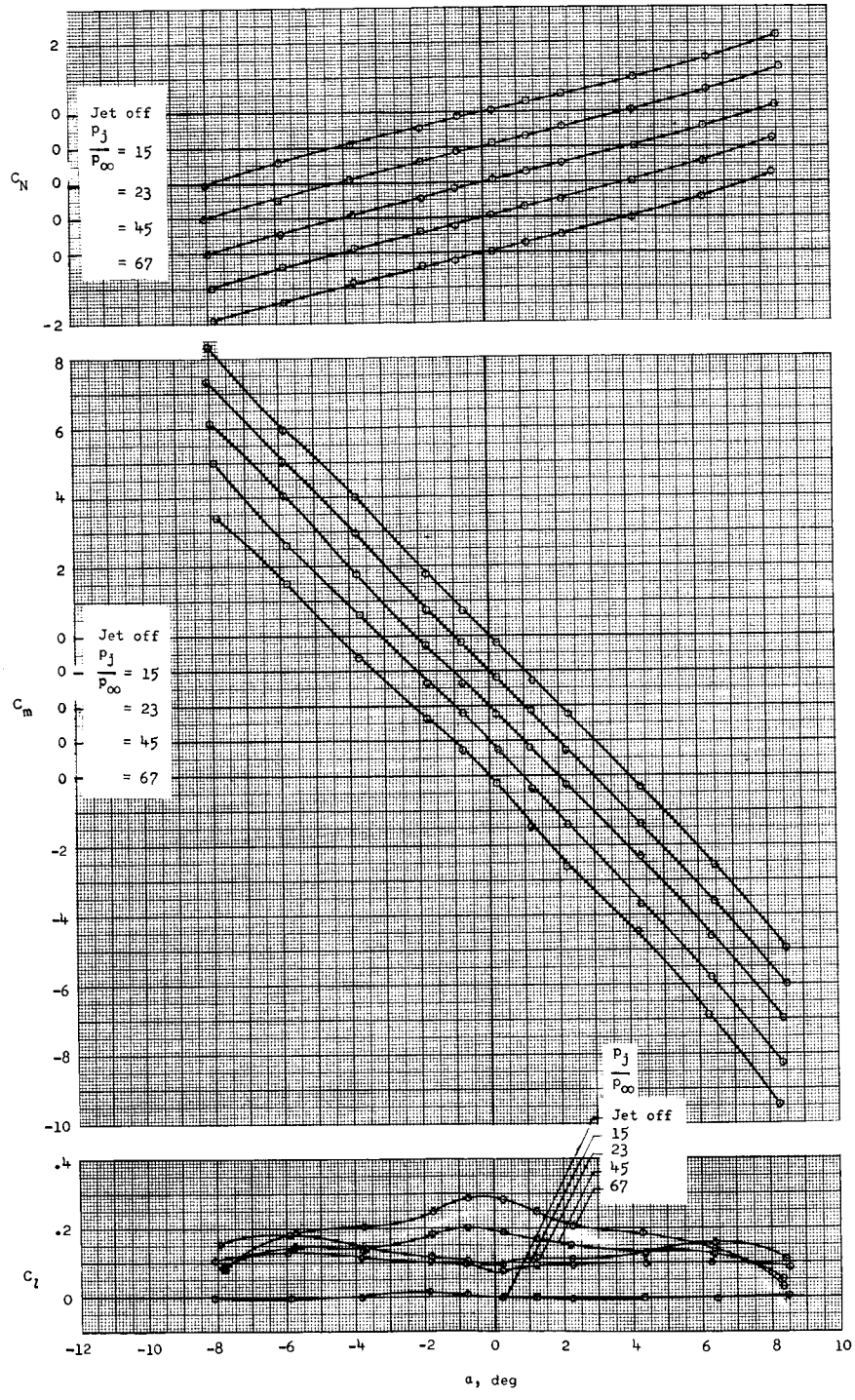

(a) Effect of p_j/p_∞ with $\delta_1 = \delta_3 = 45^0$ for negative roll-control moments and $\delta_2 = \delta_4 = 0^0$. p_j = 2450 psf (117 306 N/m^2).

Figure 5.- Effect of control-rocket exhaust and angle of attack on the aerodynamic characteristics of the complete configuration.

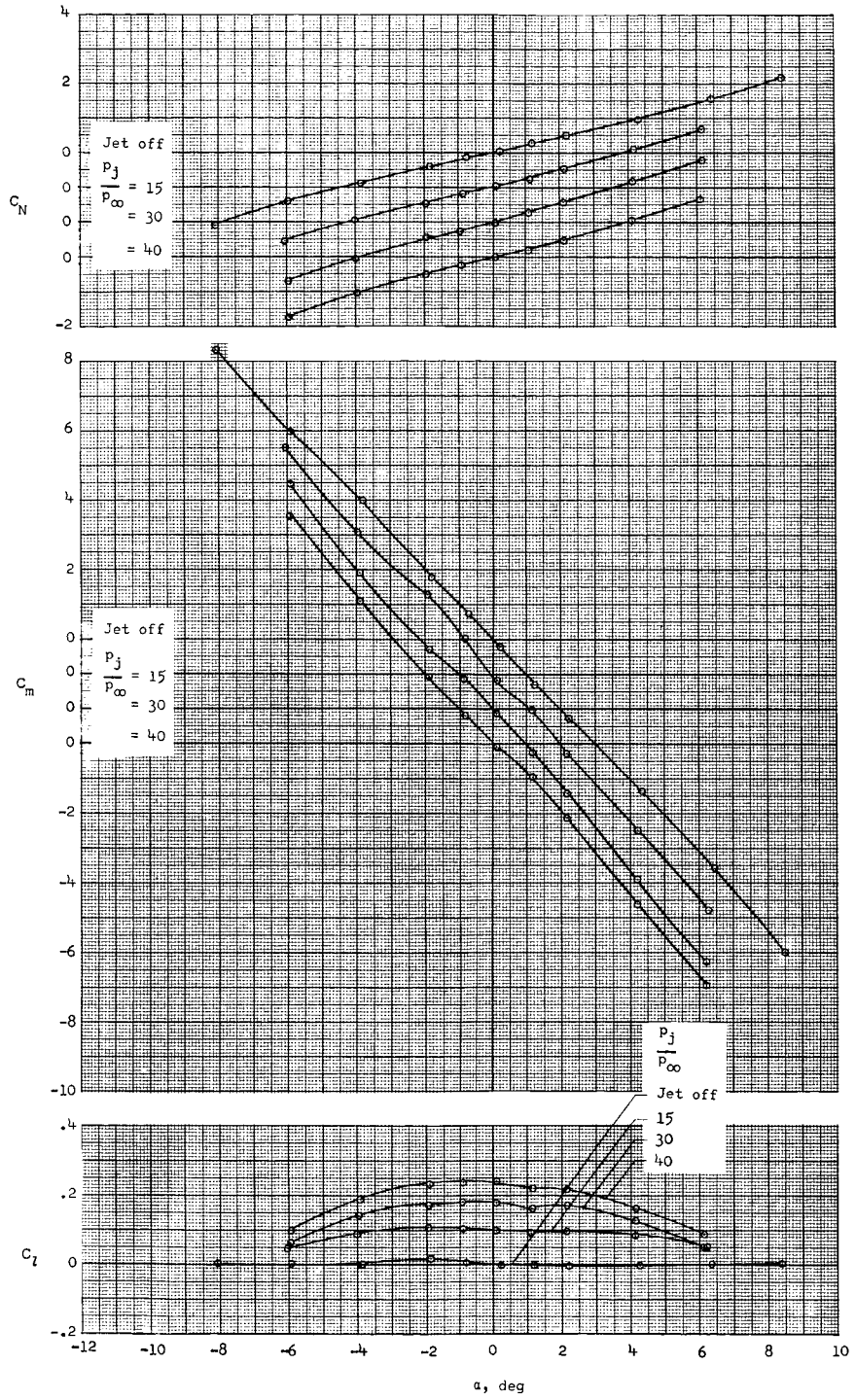

(b) Effect of p_j/p_∞ with $\delta_1 = \delta_2 = \delta_3 = \delta_4 = 30^0$ for negative roll-control moments. p_j = 1600 psf (76 608 N/m^2).

Figure 5.- Concluded.

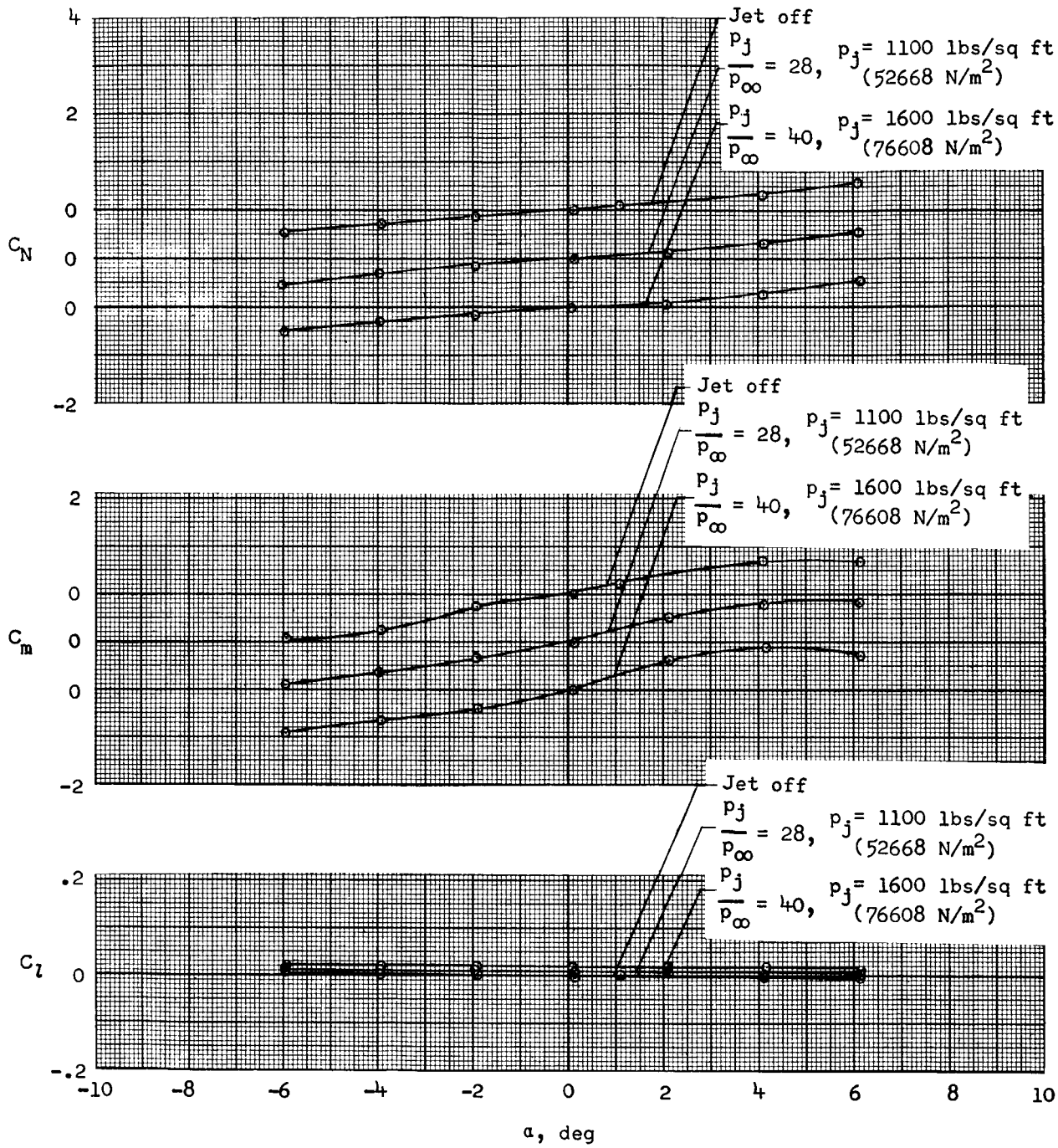

Figure 6.- Effect of control-rocket exhaust and angle of attack on aerodynamic characteristics of the configuration without auxiliary rockets and fins. $\delta_1 = \delta_3 = 45^0$ for negative roll-control moments and $\delta_2 = \delta_4 = 0^0$.

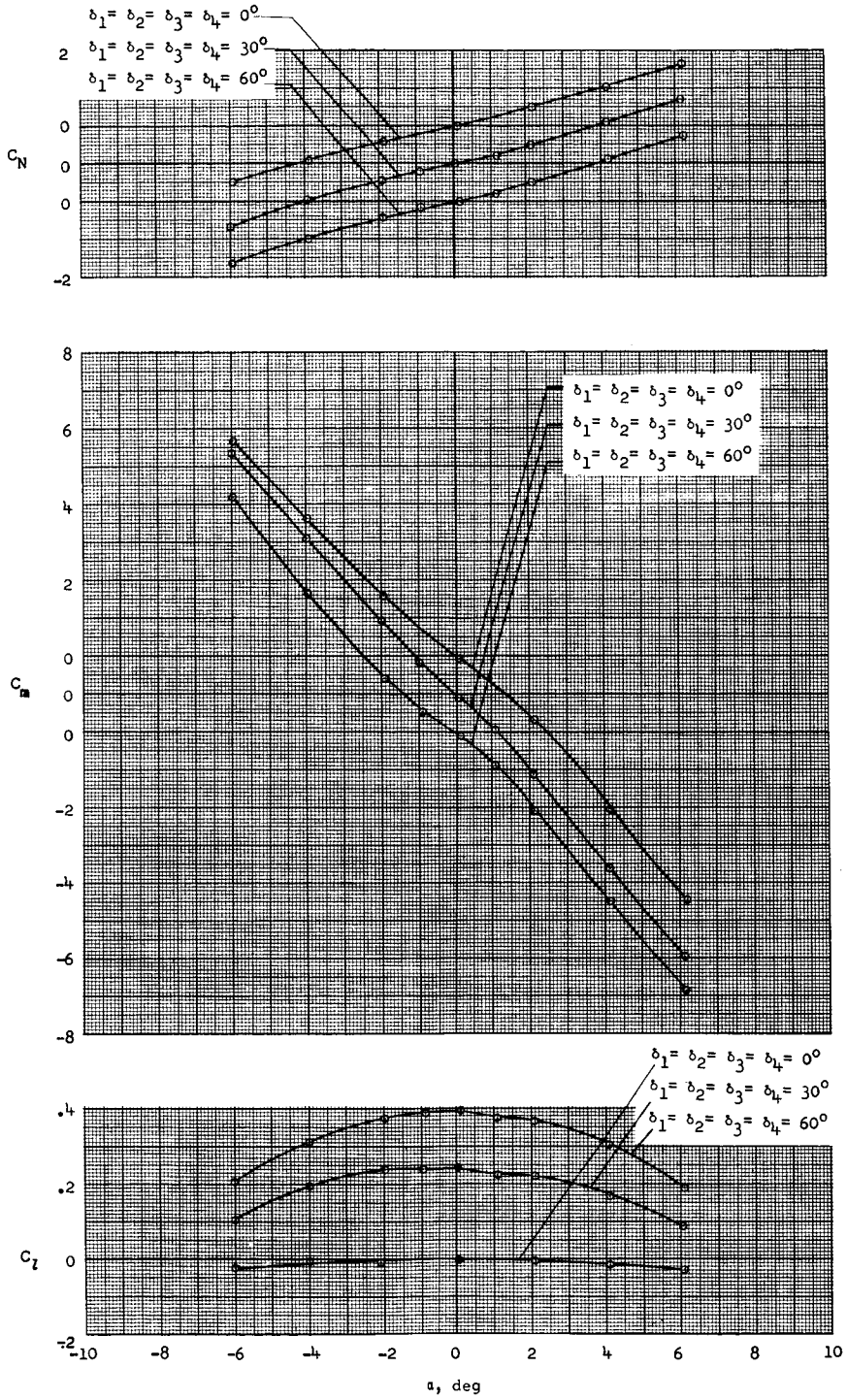

Figure 7.- Effect of roll-control deflection angle on aerodynamic characteristics of complete configuration. p_j = 1600 psf (76 608 N/m^2); p_j/p_∞ = 40 ; control deflections for negative roll moments.

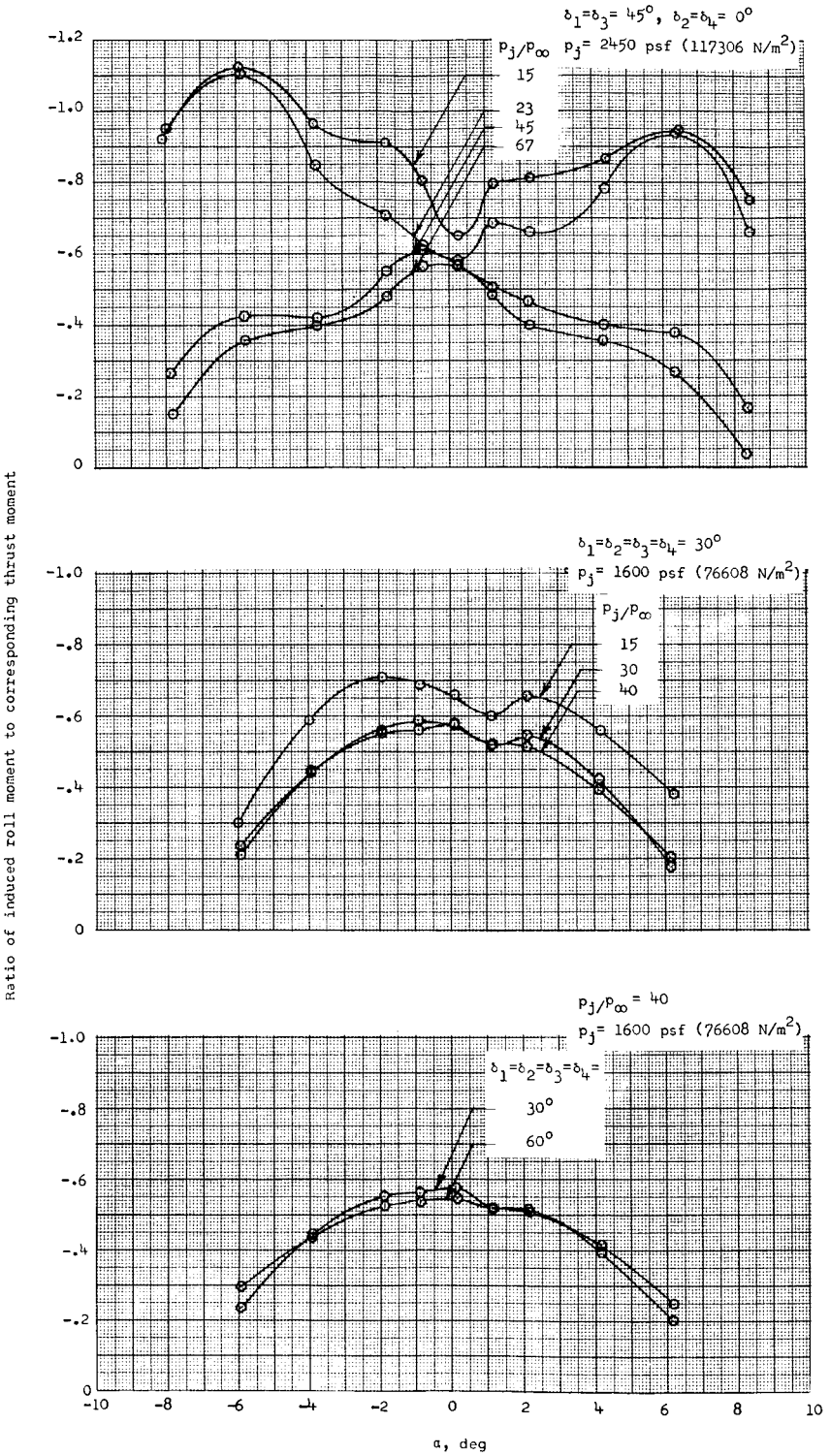

Figure 8.- Ratios of induced roll moments to applied moments for various test configurations.